

# The Bundles of Intercrossing Fibers of the Extensor Mechanism of the Fingers Greatly Influence the Transmission of Muscle Forces

Anton A Dogadov<sup>1,2</sup>, Francisco J Valero-Cuevas<sup>3</sup>, Christine Serviere<sup>1</sup>, Franck Quaine<sup>1</sup>

<sup>1</sup>Univ. Grenoble Alpes, GIPSA-Lab, F-38000 Grenoble, France

CNRS; GIPSA-Lab, F-38000 Grenoble, France

<sup>2</sup>Université Paris-Saclay, Centre National de la Recherche Scientifique, Paris-Saclay Institute of Neuroscience (NeuroPSI), Saclay, France

<sup>3</sup>Brain-Body Dynamics Lab, University of Southern California, Los Angeles, USA

**Abstract:** The extensor mechanism is a tendinous structure that plays an important role in finger function. It transmits forces from several intrinsic and extrinsic muscles to multiple bony attachments along the finger via sheets of collagen fibers. The most important attachments are located at the base of the second and third phalanges (proximal and distal attachments, respectively). How the forces from the muscles contribute to the forces at the attachment points, however, is not fully known. In addition to the well-accepted medial and lateral bands, there exist two layers of intercrossing fiber bundles (superficial interosseous medial fiber layer and deeper extensor lateral fiber layer), connecting them. In contrast to its common idealization as a minimal network of distinct strings, we built a numerical model consisting of fiber bundles to evaluate the role of multiple intercrossing fibers in the production of static finger forces. We compared this more detailed model of the extensor mechanism to the idealized minimal network that only includes the medial and lateral bands. We find that including bundles of intercrossing fibers significantly affects force transmission, which itself depends on finger posture. In a mid-flexion posture (metacarpal joint MCP = 45°; proximal interphalangeal joint PIP = 45°; distal interphalangeal joint DIP = 10°) the force transmitted by the lateral fibers is 40% lower than in a more pronounced flexed posture (MCP = 90°; PIP = 90°; DIP = 80°). We conclude that the intercrossing fiber bundles — traditionally left out in prior models since Zancolli's simplification — play an important role in force transmission and variation of the latter with posture.

**Keywords:** Finger biomechanics, Finger extensor Tendons, Extensor Apparatus, Extensor mechanism, Extensor assembly

## INTRODUCTION

The extensor mechanism of the fingers of human and non-human primates is a network of tendinous structures that drapes over the dorsum of the finger bones (Van Zwieten, 1980). It transmits forces from several extrinsic and intrinsic hand muscles to the phalanges to produce torques at the finger joints (Landsmeer, 1949). This structure plays an important role in finger function, and its disruption degrades manipulation ability. Therefore, it is usually included in detailed biomechanical models of the fingers (Hu et al., 2014; Jadelis et al., 2023; Sachdeva et al., 2015; Valero-Cuevas et al., 2007; Vaz et al., 2015). Even though the extensor mechanism is, in reality, a sheet of intersecting fibers, it has often been idealized as a sparse network of strings

38 (Chao, 1989; Garcia-Elias et al., 1991; Schultz et al., 1981; Valero-Cuevas et al., 2007; Zancolli,  
39 1979). However, the extensor mechanism is a sophisticated continuous fibrous composite  
40 structure that can be simplified as having

- 41 1. A medial band, which originates from the extrinsic *extensor digitorum communis*  
42 muscle and has its principal bone insertion at the proximal part of the middle  
43 phalanx as the proximal band (Harris and Rutledge, 1972), *i.e.* proximal extensor  
44 mechanism attachment;
- 45 2. Two lateral (or intrinsic) bands, radial and ulnar, which originate from the  
46 intrinsic muscles. The radial and ulnar bands combine and insert to the proximal  
47 part of the distal phalanx as the terminal (Harris and Rutledge, 1972), *i.e.* distal  
48 extensor mechanism attachment;
- 49 3. The intercrossing fiber bundles and the extensor hood, connecting the lateral  
50 bands with the medial one (Schultz et al., 1981) The intercrossing fiber bundles  
51 are represented by two layers of fibers: interosseous medial fibers and the  
52 extensor lateral fibers.

53 The intercrossing fibers and the extensor hood are of particular interest because they  
54 biomechanically couple the forces in the medial and terminal bands and the rotations of both  
55 interphalangeal joints (Leijnse and Spoor, 2012). Moreover, the intercrossing fibers may become  
56 more tight or slack as a function of the posture (Leijnse and Spoor, 2012), making the force  
57 transmission among the extensor mechanism bands posture dependent (Lee et al., 2008;  
58 Sarrafian et al., 1970). This biomechanical coupling has been interpreted as also enabling a  
59 nonlinear transmission of tendon forces (*i.e.*, a “switch” behavior) that improves controllability  
60 under the anatomical constraints that the fingers do not have any muscles in them (Valero-  
61 Cuevas et al., 2007). This means that changing the ratio between the input forces from the  
62 intrinsic and extrinsic muscles itself changes the distribution of forces across the proximal and

63 terminal bands. However, we lack detailed studies identifying the posture-dependent interactions  
64 by which the multiple fiber bundles of the extensor mechanism enables finger function.

65 The purpose of this study is to fill this gap in understanding by using a more detailed  
66 model of the fiber bundles of the extensor mechanism to understand the role of the extensor hood  
67 and the intercrossing fibers on muscle force transmission to produce static fingertip force. In the  
68 current study, we focus, without loss of generality, on the extensor mechanism of the middle  
69 finger. Applied to the middle finger, the intrinsic muscles, mentioned above, are the second and  
70 the third dorsal interosseous muscles, and the second lumbrical muscle. In particular, we built  
71 and compared two three-dimensional models of the extensor mechanism: a more detailed model  
72 that includes the intercrossing fibers and an extensor hood, and a trivial model, without any  
73 structures connecting the central band with the lateral bands. We call it the “trivial” model  
74 because it reflects the theoretical baseline architecture of muscles where tendons originate in a  
75 muscle and insert into bone. While we do not endorse such a trivial structure, this trivial model is  
76 not a straw man. Rather, it is the baseline musculotendon anatomy, which evolutionary  
77 pressures—presumably of biomechanical nature—drove to specialize into an extensor  
78 mechanism. As such, it does help highlight and quantify the biomechanical benefits of a  
79 sophisticated extensor mechanism where tendons that originate in muscle combine with other  
80 tendons to then insert into bone.

81 Our results demonstrate changes in force transmission with changes in posture,  
82 introduced by the extensor hood and the intercrossing fiber bundles. The functional differences  
83 compared to the trivial model speaks to the evolutionary pressures that may have driven the  
84 evolution of the topology of the extensor mechanism in the first place, given the anatomical  
85 constraints that the fingers do not have any muscles in them and must be actuated by muscles in  
86 the palm and forearm. Our model simulating muscle force transmission via bundles of  
87 intercrossing fibers now allows us to better understand neuromuscular strategies for finger  
88 control, and explain the functional deficits associated with clinically common ruptures or

89 adhesions of the elements of the extensor mechanism. It also enables the design of prostheses  
90 and robotics hands using such interconnected tendon architectures.

## 91 **METHODS**

92 We coded a custom numerical environment that allows representing the extensor  
93 mechanism as contacting bundles of interconnecting fibers. Each string or consists of a sequence  
94 of points, pairwise connected by elastic elements with a linear stress-strain model. This  
95 computational environment is written using Matlab 2015 and C++, and is based on the extensor  
96 mechanism simulator, described in detail elsewhere (Dogadov et al., 2017). This environment  
97 allows simulating tendinous structures with arbitrary topologies and finger postures for static  
98 analysis. For a given vector of input muscle forces, it calculates the resulting net joint torques  
99 and fingertip wrench (endpoint forces and torques).

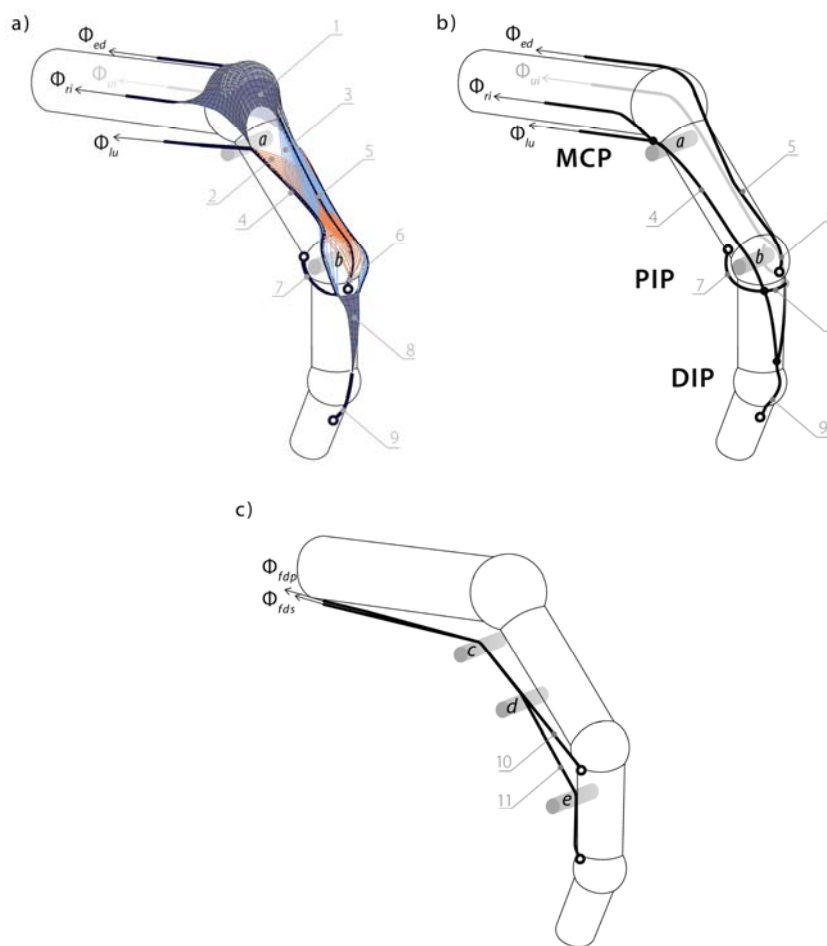
100 The first model (Fig. 1a) was a full extensor mechanism model that includes multiple  
101 bundles of intercrossing fibers to approximate the known anatomical bands and sheets of  
102 collagenous tissue. The model contains medial band (5), connecting the extrinsic *extensor*  
103 *digitorum* muscle with the proximal band (6). The latter forms a proximal attachment of the  
104 extensor mechanism to the skeleton. The model also contains the lateral (or interosseous) bands  
105 (4), connecting the intrinsic muscles with terminal band (9). The latter forms a distal attachment  
106 of the extensor mechanism to the skeleton. The attachment points of the tendons and ligaments  
107 to bones are shown by circles. Finally, the model contains the structures connecting the lateral  
108 band with the medial one. These structures are the extensor hood (1) and the bundles of  
109 intercrossing fibers: the interosseus medial fibers (2, shown in red) and the extensor lateral fibers  
110 (3, shown in blue). These bundles are shown enlarged in Fig. 2.

111 The second model was the baseline (trivial) one (Fig. 1b), with no structures, connecting  
112 the lateral tendons with the medial one, *i.e.* it does not contain the extensor hood and  
113 intercrossing fiber bundles. The transverse retinacular ligament (7) and triangular ligament (8)

114 were included to both models as they are needed to maintain tendon alignment and prevent  
115 bowstringing during force transmission.

116 Finally, Fig. 1c shows the tendons from the flexor muscles, *flexor digitorum superficialis*  
117 (FDS) and *flexor digitorum profundus*, (FDP). Both the full and trivial models included the same  
118 tendons from the flexor muscles. We do not include any connection between the flexor tendons  
119 and the extensor mechanism.

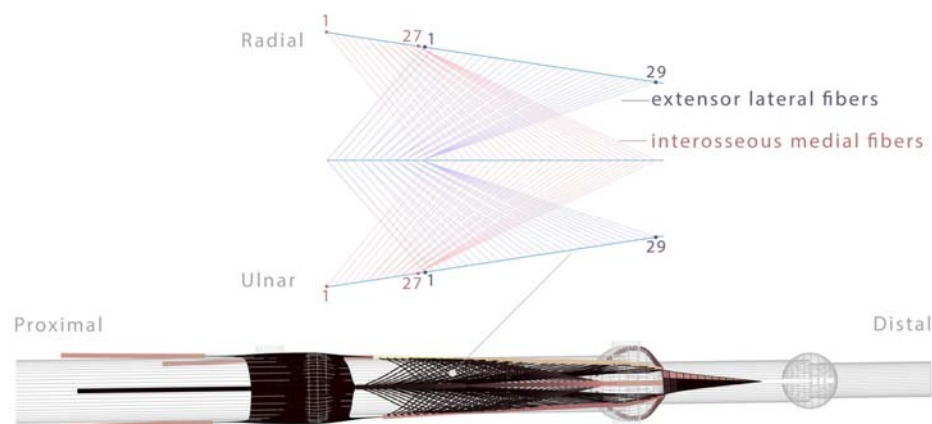
120



121

122 *Fig. 1. The view of the extensor mechanism modelled in a developed environment. a: the full model, which contains*  
123 *the principal tendon and ligaments of the extensor mechanism: 1 – the extensor hood, 2 – interosseous medial fibers*  
124 *(red), 3 – the extensor lateral fibers (blue), 4 – lateral band, 5 – medial band, 6 – proximal band, 7 – transverse*  
125 *retinacular ligament, 8 – triangular ligament, 9 – terminal band. b: the trivial model. The trivial model does not*  
126 *contain the structures connecting the lateral bands (4) with the extensor medial band (5). c: flexor tendons: 10 –*  
127 *flexor digitorum superficialis tendon, 11 – flexor digitorum profundus tendon (same for both models)*

128 Each extensor mechanism model was draped over on the finger bones in an initial  
129 configuration according to anatomical data (Garcia-Elias et al., 1991). The model of the bony  
130 anatomy included the metacarpal bone, proximal, middle and distal phalanx of the middle finger.  
131 The finger joints considered in the model are a metacarpal (MCP; flexion-extension and ad-  
132 abduction), proximal interphalangeal (PIP; flexion-extension), and distal interphalangeal (DIP;  
133 flexion-extension) joints. The bones were represented as ideal cylinders capped by spheres. The  
134 geometric parameters of the cylinders and spheres were based on anatomical surveys (Buchholz  
135 et al., 1992; Darowish et al., 2015) to be, respectively: cylinder lengths 64.6 mm, 44.6 mm,  
136 26.3 mm, 17.4 mm; cylinder radii 4.5 mm, 4.0 mm, 3.0 mm, 2.5 mm; the sphere radii 5.0 mm,  
137 5.4 mm, 4 mm for both models.



138

139 *Fig. 2. The schematic view of the intercrossing fibers. Red: interosseous medial fibers; blue: extensor lateral fibers.*

140 In addition to bones, five cylinders (a-e in Fig. 1) with smaller radii were included to the  
141 model to avoid tendon bowstringing. The cylinder a is perpendicular to the metacarpal bone and  
142 replaces a presumed function of the lumbrical muscle pulley (Stack, 1963); the cylinder b is  
143 perpendicular to proximal phalanx bone and replaces the presumed function of the protuberances  
144 of  $p_1$  head. Cylinders  $c$ ,  $d$ ,  $e$  simulate the annular pulleys that prevent bowstringing of the flexor  
145 tendons.

146 The force of the *extensor digitorum communis* muscle (EDC), ulnar and radial  
147 *interosseous* muscle (UI, RI), and lumbrical muscle (LU) were applied to the extensor  
148 mechanism model as the input forces. We will note the muscle force values as vector  $\Phi$ :

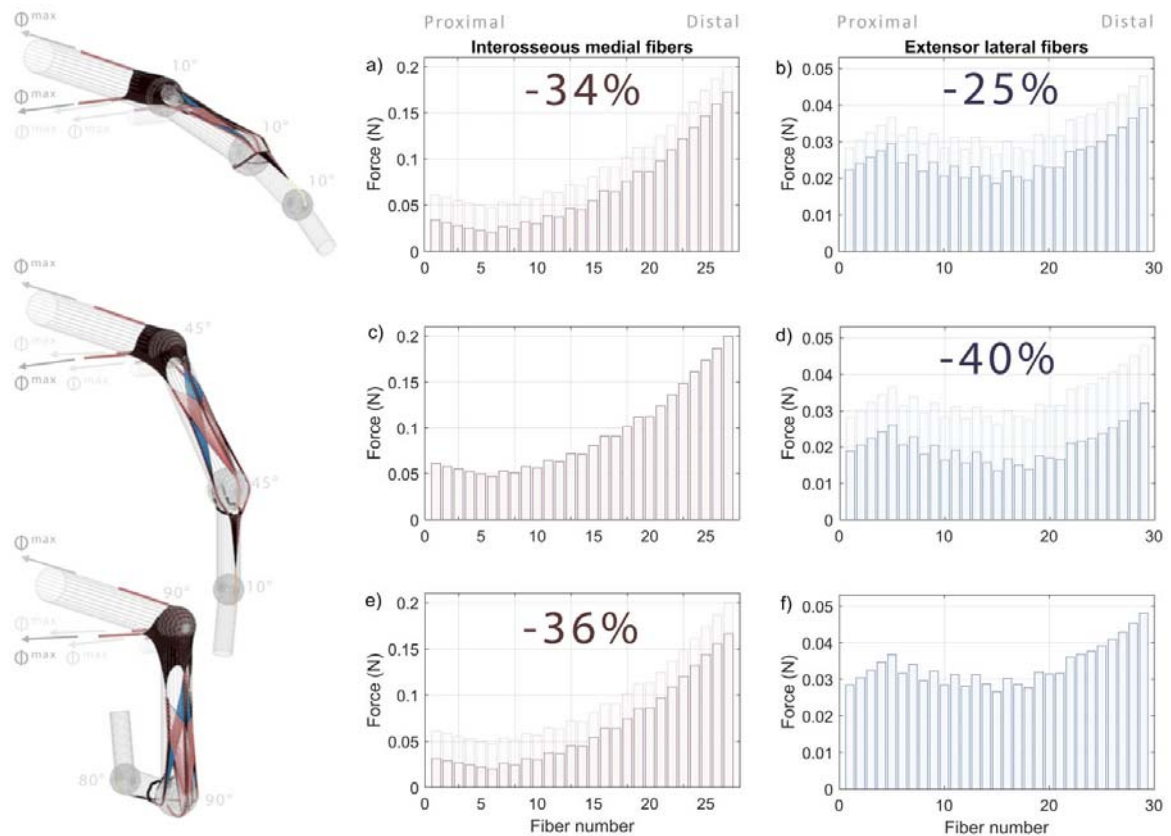
149 
$$\Phi = [\Phi_{ed} \ \Phi_{ui} \ \Phi_{ri} \ \Phi_{lu}]^T.$$

150 The deformation of the extensor mechanism due to the applied forces and geometric  
151 constraints imposed by the bones and the cylinders  $a, b$  was performed to minimize the overall  
152 potential energy (i.e., strain as in (Valero-Cuevas and Lipson, 2004)) of all elastic elements by a  
153 gradient algorithm until the equilibrium state was found, as described in (Dogadov et al., 2017).

154 Once the equilibrium state of the extensor mechanism was found for a set of applied  
155 forces, the tendon tensions internal to the extensor mechanism and resulting force at the  
156 insertions can be read out. The tensions for each element of the deformed extensor mechanism  
157 are found by multiplying its elongation by its stiffness. The forces, transmitted from the extensor  
158 mechanism to the bones, including the forces in tendinous insertions and contact forces (the  
159 reaction forces created by the tendons overlapping the bones), are used to calculate net joint  
160 torques. The torque created by the extensor mechanism were calculated at each kinematic degree  
161 of freedom (two for MCP and one each for PIP and PIP). The output fingertip wrench was found  
162 as a product of the finger Jacobian inverse transpose, defined by the finger geometry and a  
163 posture, with the joint torque vector. This approach is explained in (Valero-Cuevas, 2015;  
164 Valero-cuevas et al., 1998).

165 **RESULTS**

166 Fig. 3 shows the force distribution among the extensor mechanism intercrossing fiber  
167 bundles with the posture. The forces in bundles from both side of the finger were similar;  
168 therefore, Fig. 3 shows only the forces in the fiber layers from the radial side of the finger. The  
169 fiber numbers in Fig. 3 are the same as in Fig. 2. In each posture the extensor mechanism was  
170 loaded by four constant muscle forces (UI, EDC, RI, and LU), each of 2.9 N.



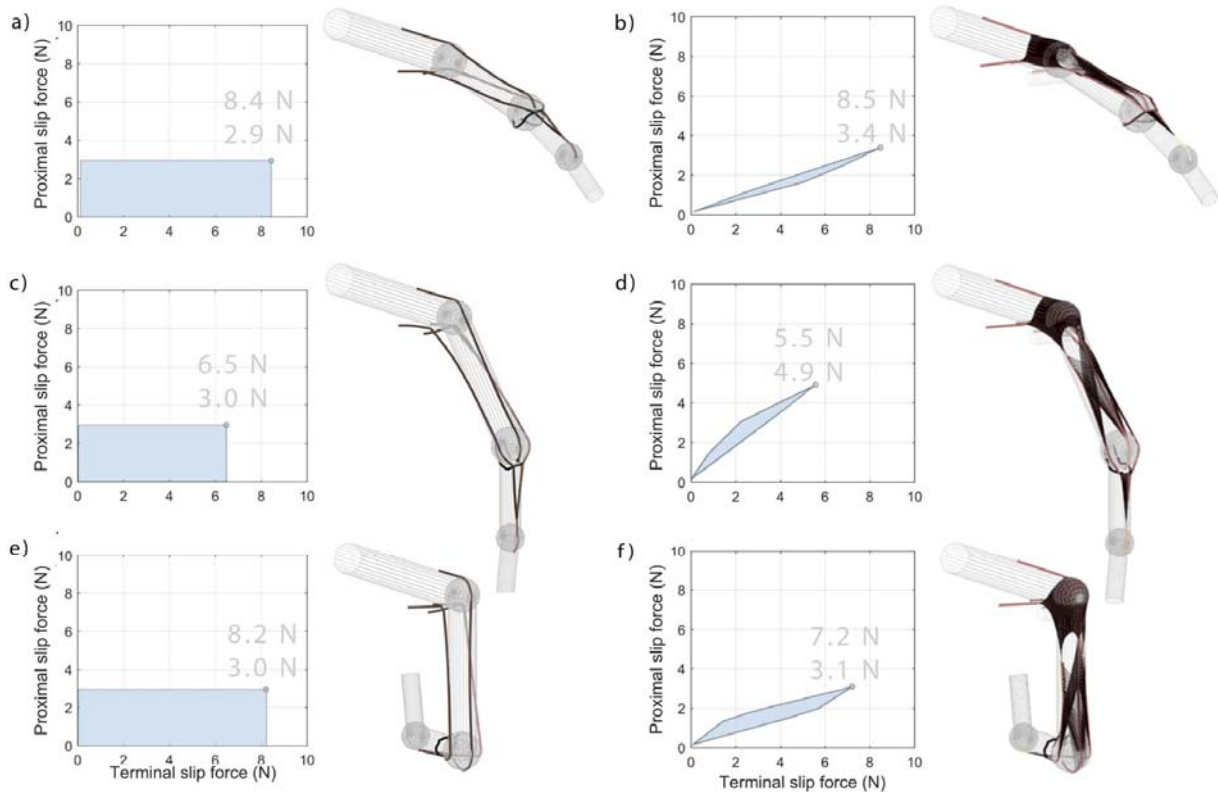
171

172 *Fig. 3. The influence of the posture on the forces forces in intercrossing fiber bundles. Red: interosseous medial fibers; blue:*  
173 *extensor lateral fibers. The first row corresponds to extension (MCP = 10°, PIP = 10°; DIP = 10°), the second row corresponds*  
174 *to mid-flexion (MCP = 45°, PIP = 45°; DIP = 10°), and the third row corresponds to flexion (MCP = 90°, PIP = 90°; DIP =*  
175 *80°). The input forces were 2.9 N in UI, EDC, RI and LU muscle for all postures. The maximal value of forces in interosseous*  
176 *medial fibers was attained in mid-flexion and the maximal value in extensor lateral fibers was attained in full flexion.*

177           It may be seen from the figure that the forces in intercrossing fiber bundles vary with the posture  
178 for a constant input force vector. The force in interosseous medial fibers (shown in red) attained the  
179 maximal value in mid-flexion posture. The mean force, calculated over all interosseous medial fibers in  
180 this posture was 34% higher than in extension and 36% higher than in flexion (0.67 N, 0.66 N and 0.94 N  
181 for extension, flexion and mid-flexion correspondingly). The forces in extensor lateral fibers arrived to  
182 maximal value in flexion posture. The mean force, calculated over all extensor lateral fibers was 25%  
183 higher in this posture than in extension and 40% higher than in mid-flexion (0.25 N, 0.20 N and 0.31 N  
184 for extension, mid-flexion and flexion correspondingly).

185

186 Fig. 4 shows the changes in the feasible tendon force set of the full extensor mechanism model  
187 (right column) in comparison with a trivial model (left column). The full-loading state, which was the  
188 state when all four extensor muscle forces were equal to  $\Phi^{\max}$ , is shown by a circle in each panel.  
189



190

191 *Fig. 4. The effect of the posture on feasible tendon force set. Left column corresponds to a trivial extensor mechanism model,*  
192 *right column corresponds to a full model. The first row corresponds to extension (MCP = 10°; PIP = 10°; DIP = 10°), the*  
193 *second row corresponds to mid-flexion (MCP = 45°; PIP = 45°; DIP = 10°), and the third row corresponds to flexion posture*  
194 *(MCP = 90°; PIP = 90°; DIP = 80°). The full-loading state, which corresponds to loading of the extensor mechanism models by*  
195 *all four muscles, is shown by a circle in each feasible tendon force set. The proximal and terminal band force values in full-*  
196 *loading state are comparable for both models, but the areas of the feasible tendon force set are smaller for the full model. Also*  
197 *for a full model, the shape and orientation of the feasible tendon force set change with posture*

198

199 It can be seen from the left column of the image, that the feasible tendon force set of the  
200 trivial model had a rectangular shape for all postures. The maximal force in proximal band did  
201 not change significantly with posture and was equal to 2.9 N in extension and to 3.0 N in other  
202 postures. The maximal force in terminal band was similar in extension and flexion (8.4 N and 8.2  
203 N), but decreased in mid-flexion (6.5 N). This may be explained by the fact that force in terminal  
204 tendon is controlled by lateral bands, which are connected by a triangular membrane. Stretching  
of the triangular membrane in flexion may influence the terminal band force. The ratio between

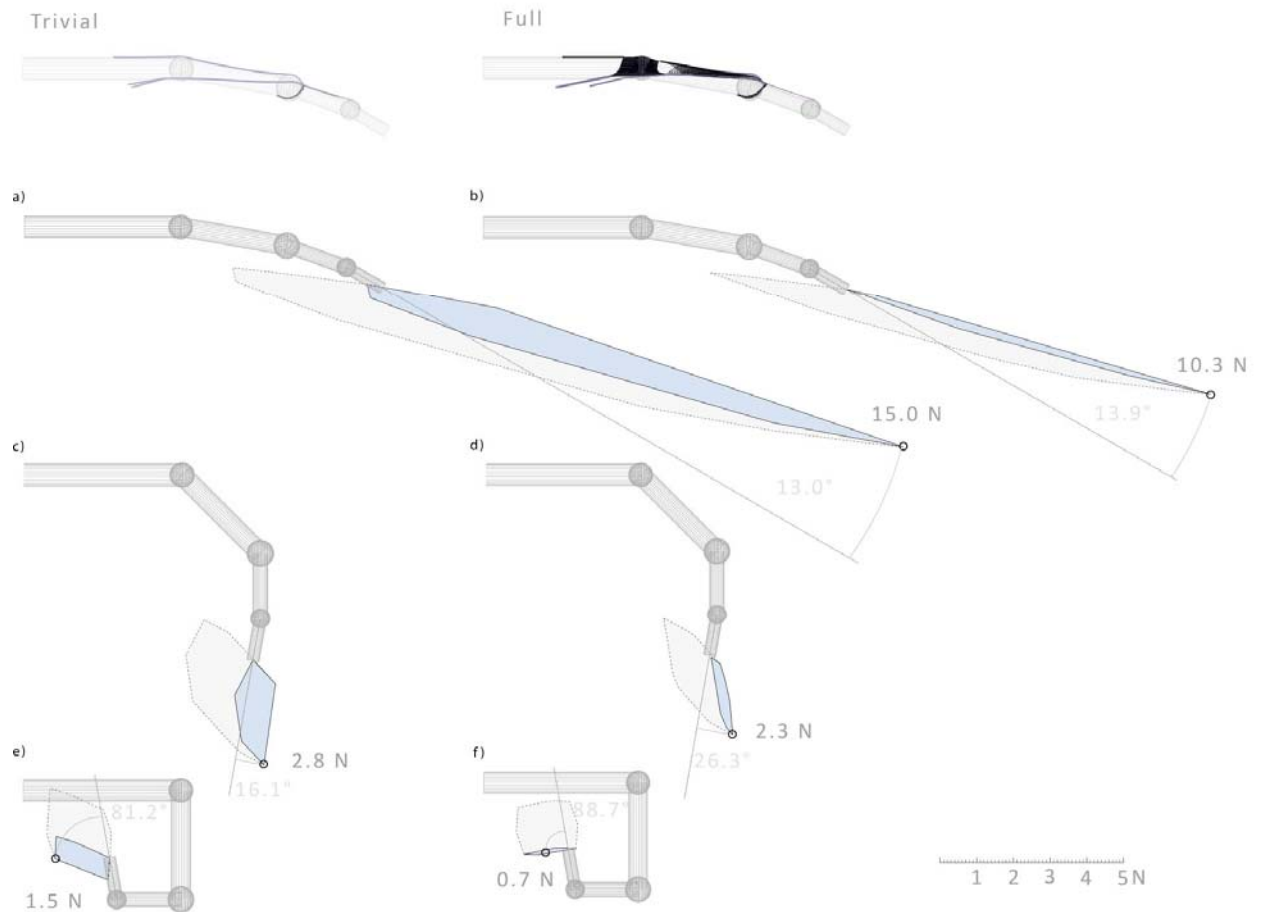
205 the force in proximal and terminal band of the trivial extensor mechanism model in full-loading  
206 state was 0.35 in extension, 0.46 in mid-flexion and 0.37 in flexion.

207 Contrary to trivial model, the shape, size, and orientation of the feasible tendon force set  
208 of the full model strongly change with posture. When the model was loaded by all muscle forces,  
209 the force in the proximal band achieved the maximal value in mid-flexion, which was 44%  
210 higher than in extension and 58% higher than in flexion (4.9 N, 3.4 N, and 3.1 N for mid-flexion,  
211 extension and flexion correspondingly). Contrary to proximal band, the force in terminal band  
212 arrived to a minimal value in mid-flexion, which was 35% lower than in extension and 24%  
213 lower than in flexion (5.5 N, 8.5 N, and 7.2 N for mid-flexion, extension and flexion  
214 correspondingly). As the result of the fact, that the force in proximal and terminal band change  
215 differently with posture, the ratio between the force in proximal and terminal band in a full-  
216 loading state also varied with posture, and was equal to 0.40 in extension posture, which was the  
217 minimal value among all postures. This ratio was maximal in mid-flexion and was equal to 0.89.  
218 In flexion, this ratio was equal to 0.43, which is close to the value in extension. It can be also  
219 noticed that the area of the feasible tendon forces set for full model was lower than the  
220 corresponding areas of the for the trivial model (*e.g.* for the extended finger area of the feasible  
221 tendon force set for full model was 9% of the feasible tendon force set for trivial model at the  
222 same posture).

223 Fig. 5 shows the effects of the posture on x-y plane projections of the feasible fingertip  
224 force set (FFS). The left column corresponds to the trivial extensor mechanism model, the right  
225 column to the full extensor mechanism model. The full-loading fingertip force, which was  
226 produced by the model when all four extensor muscle forces were equal to  $\Phi^{\max}$ , is shown by a  
227 circle in each panel. The dark blue area corresponds to the forces created only by the muscles,  
228 attached to the extensor mechanism (UI, EDC, RI, and LU) and with no forces in flexor muscles.  
229 The light area stands for the forces, created when the flexor muscles were also active (FDS,

230 FDP). For both trivial and full model, shape and orientation of FFS changes with posture were  
 231 observed.

232



233

234 *Fig. 5. Influence of the posture on x-y plane projection of the feasible force set. Left column corresponds to a trivial extensor*  
 235 *mechanism model, right column corresponds to a full model. First row corresponds to extension posture (MCP = 10°;*  
 236 *PIP = 10°; DIP = 10°), second row corresponds to mid-flexion posture (MCP = 45°; PIP = 45°; DIP = 10°), third row*  
 237 *corresponds to flexion posture (MCP = 90°; PIP = 90°; DIP = 80°). The area of the feasible force set as well as fingertip force*  
 238 *values in full-loading state are smaller for full extensor mechanism model for all postures. Blue area corresponds to a subset in*  
 239 *a feasible force set produced only by the muscles, attached to the extensor mechanism (UI, EDC, RI, and LU)*

240

241 The x-y plane projection of the full loading force is lower for the full model than for  
 242 trivial model for all postures. The full-loading force in full model is 31% lower than in trivial  
 243 model in extension (10.3 N and 15.0 N correspondingly), 18% lower in mid-flexion (2.3 N and  
 244 2.8 N), and 53% lower in flexion (0.7 N and 1.5 N). The angle between the distal phalanx and  
 245 the xOy-projection of the full-loading force is higher in full model than in trivial one. In  
 extension, the angle in full model and trivial model are 13.9° and 13.0° correspondingly, in mid-

246 flexion the angles are  $26.3^\circ$  and  $16.1^\circ$  and in full flexion the angles are  $88.7^\circ$  and  $81.2^\circ$ . Finally,  
247 it can be also noticed from the figure that the area of the FFS of the full extensor mechanism  
248 model is lower than the area of the FFS of the trivial model.

249

250

## DISCUSSION

251 We demonstrated that the intercrossing fiber bundles and the extensor hood reduces the  
252 area of feasible tendon force set the full extensor mechanism model, which contain the  
253 intercrossing fibers and the extensor hood, is lower than the areas of feasible tendon force set and  
254 FFSs, produced by the trivial model, in which there are no connections between the medial and  
255 lateral bands. This area increases due to the fact that the trivial extensor mechanism model  
256 enables the independent control of the forces in the proximal and terminal band. However, in the  
257 case of the full model of the extensor mechanism, these forces are naturally coupled.

258 Secondly, we have shown that the bundles of intercrossing fiber can modify the force  
259 distribution according to posture. This may indicate that the nervous system has to modulate the  
260 sharing in involved muscle and intensity according to the finger posture in order to produce the  
261 wanted fingertip force. This may imply that there exists a link between the passive adaptations of  
262 the extensor mechanisms and the active modulation of the muscle recruitments for useful  
263 fingertip tasks, such as grasping objects (Wei et al., 2022), writing (Gerth and Festman, 2023), or  
264 playing musical instrument (Furuya et al., 2011).

265 The analyzed full model has several limitations. Firstly, the model topology  
266 oversimplifies the real extensor mechanism anatomy. Over MCP joint the extensor mechanism  
267 was represented only by the extensor hood. However, the metacarpophalangeal fibrous griddle,  
268 or sagittal band, which connect the extensor tendons to the deep transverse intermetacarpal  
269 ligament and capsular joint (Zancolli, 1979) was not taken into account. Moreover, no  
270 attachments of the extensor mechanism at the base of the proximal phalanx were taken into

271 account. Secondly, the bones were modeled as cylinders with spheres corresponding to the  
272 joints.

273 This study is limited in that it does not include all other muscles acting on the finger, but  
274 this work enables future work to understand the function of the human fingers that considers  
275 their complex anatomy in more detail.

276 In addition, this work only considered force transmission by the trivial model, but does  
277 not consider other important biomechanical consequences of it. First and foremost is the need to  
278 maintain and regulate the tendon path as the finger changes posture, where the “unsupported”  
279 trivial tendons may slide, bowstring, cause rapid changes in moment arms and even cause  
280 tendinitis or scarring during their unguided sliding movement. In our model, the path of the  
281 tendons in the trivial model was enforced arbitrarily. From this perspective, the extensor  
282 mechanism may serve to retain force transmission while also serving as a support and guiding  
283 structure, much like the annular bands and sesamoids in other tendons.

284 And secondly, there are other considerations in addition to tendon force and joint torque  
285 production. Recent work has suggested that tendon force transmission is important for other  
286 important aspects of function such as stability during force production (Sharma and Venkadesan,  
287 2022). Similarly, producing slow finger movements very likely depend more on managing the  
288 internal strain energy of the system and not second-order rigid-body dynamics driven by joint  
289 torques or muscle forces (Babikian et al., 2016).

290 As such, the evolutionary pressures for the formation of the extensor mechanism may not  
291 be strictly limited to force transmission. That is, the extensor mechanisms may have been a  
292 multi-factorial evolutionary adaptation that also allows for stability and accurate slow  
293 movements with the fingertips that gave human-primates a competitive advantage for effective  
294 manipulation capabilities.

295 **ACKNOWLEDGEMENTS**

296 The work was supported by IDEX scholarship for international mobility. The author  
297 acknowledge Vishweshwer Shastri (USC) and Gelu Ionescu (GIPSA-Lab) for their assistance  
298 with the programming of the extensor mechanism simulator.

## 299 REFERENCES

- 300 Babikian, S., Valero-Cuevas, F.J., Kanso, E., 2016. Slow Movements of Bio-Inspired Limbs. *J.*  
301 *Nonlinear Sci.* 26, 1293–1309. <https://doi.org/10.1007/s00332-016-9305-x>
- 302 Buchholz, B., Armstrong, T.J., Goldstein, S.A., 1992. Anthropometric data for describing the  
303 kinematics of the human hand. *Ergonomics* 35, 261–273.  
304 <https://doi.org/10.1080/00140139208967812>
- 305 Chao, E.Y., 1989. *Biomechanics of the Hand: A Basic Research Study.* World Scientific.
- 306 Darowish, M., Brenneman, R., Bigger, J., 2015. Dimensional analysis of the distal phalanx with  
307 consideration of distal interphalangeal joint arthrodesis using a headless compression screw.  
308 *Hand* 100–104. <https://doi.org/10.1007/s11552-014-9679-x>
- 309 Dogadov, A., Alamir, M., Serviere, C., Quaine, F., 2017. The biomechanical model of the long  
310 finger extensor mechanism and its parametric identification. *J. Biomech.* 58.  
311 <https://doi.org/10.1016/j.jbiomech.2017.04.030>
- 312 Furuya, S., Flanders, M., Soechting, J.F., 2011. Hand kinematics of piano playing. *J.*  
313 *Neurophysiol.* 106, 2849–2864. <https://doi.org/10.1152/jn.00378.2011>
- 314 Garcia-Elias, M., An, K.N., Berglund, L., Linscheid, R.L., Cooney, W.P., Chao, E.Y., 1991.  
315 Extensor mechanism of the fingers. I. A quantitative geometric study. *J. Hand Surg. Am.*  
316 16, 1130–1136. [https://doi.org/10.1016/S0363-5023\(10\)80079-6](https://doi.org/10.1016/S0363-5023(10)80079-6)
- 317 Gerth, S., Festman, J., 2023. Muscle Activity during Handwriting on a Tablet: An  
318 Electromyographic Analysis of the Writing Process in Children and Adults. *Children* 10.  
319 <https://doi.org/10.3390/children10040748>

- 320 Harris, C., Rutledge, G.L., 1972. The functional anatomy of the extensor mechanism of the  
321 finger. *J. Bone Joint Surg. Am.* 54, 713–726. [https://doi.org/10.1097/00006534-197301000-](https://doi.org/10.1097/00006534-197301000-00039)  
322 00039
- 323 Hu, D., Ren, L., Howard, D., Zong, C., 2014. Biomechanical Analysis of Force Distribution in  
324 Human Finger Extensor Mechanisms. *Biomed Res. Int.* 2014.
- 325 Jadelis, C.T., Ellis, B.J., Kamper, D.G., Saul, K.R., 2023. Cosimulation of the index finger  
326 extensor apparatus with finite element and musculoskeletal models. *J. Biomech.* 157,  
327 111725. <https://doi.org/10.1016/j.jbiomech.2023.111725>
- 328 Landsmeer, J.M.F., 1949. The anatomy of the dorsal aponeurosis of the human finger and its  
329 functional significance. *Anat. Rec.* 104, 31–44. <https://doi.org/10.1002/ar.1091040105>
- 330 Lee, S.W., Chen, H., Towles, J.D., Kamper, D.G., 2008. Estimation of the effective static  
331 moment arms of the tendons in the index finger extensor mechanism. *J. Biomech.* 41, 1567–  
332 1573. <https://doi.org/10.1016/j.jbiomech.2008.02.008>
- 333 Leijnse, J.N. a L., Spoor, C.W., 2012. Reverse engineering finger extensor apparatus  
334 morphology from measured coupled interphalangeal joint angle trajectories - a generic 2D  
335 kinematic model. *J. Biomech.* 45, 569–578. <https://doi.org/10.1016/j.jbiomech.2011.11.002>
- 336 Sachdeva, P., Sueda, S., Bradley, S., Fain, M., Pai, D.K., 2015. Biomechanical simulation and  
337 control of hands and tendinous systems. *ACM Trans. Graph.* 34, 42:1-42:10.  
338 <https://doi.org/10.1145/2766987>
- 339 Sarrafian, S.K., Kazarian, L.E., Topouzian, L.K., Sarrafian, V.K., Siegelman, A., 1970. Strain  
340 variation in the components of the extensor apparatus of the finger during flexion and  
341 extension. A biomechanical study. *J. Bone Joint Surg. Am.* 52, 980–990.
- 342 Schultz, R., Furlong II, J., Storace, A., 1981. Detailed anatomy of the extensor mechanism at the  
343 proximal aspect of the finger. *J. Hand Surg. Am.* 6, 493–498. <https://doi.org/7276481>

- 344 Sharma, N., Venkadesan, M., 2022. Finger stability in precision grips. *Proc. Natl. Acad. Sci. U.*  
345 *S. A.* 119, 1–9. <https://doi.org/10.1073/pnas.2122903119>
- 346 Stack, H.G., 1963. A study of muscle function in the fingers. *Ann. R. Coll. Surg. Engl.* 33, 307–  
347 322.
- 348 Valero-Cuevas, F.J., 2015. *Fundamentals of Neuromechanics, Biosystems & Biorobotics.*  
349 Springer London, London. <https://doi.org/10.1007/978-1-4471-6747-1>
- 350 Valero-cuevas, F.J., Anand, V. V, Saxena, A., Lipson, H., 2007. Beyond Parameter  
351 Estimation □: Extending Biomechanical Modeling by the Explicit Exploration of Model  
352 Topology 54, 1951–1964.
- 353 Valero-Cuevas, F.J., Lipson, H., 2004. A computational environment to simulate complex  
354 tendinous topologies. *Conf. Proc. IEEE Eng. Med. Biol. Soc.* 6, 4653–4656.  
355 <https://doi.org/10.1109/IEMBS.2004.1404289>
- 356 Valero-Cuevas, F.J., Yi, J.W., Brown, D., McNamara, R. V., Paul, C., Lipson, H., 2007. The  
357 tendon network of the fingers performs anatomical computation at a macroscopic scale.  
358 *IEEE Trans. Biomed. Eng.* 54, 1161–1166. <https://doi.org/10.1109/TBME.2006.889200>
- 359 Valero-cuevas, F.J., Zajac, F.E., Burgar, C.G., 1998. Large index-fingertip forces are produced  
360 by subject-independent patterns of muscle excitation 31.
- 361 Van Zwieten, K.J., 1980. Some functional-anatomical characteristics of finger movements in the  
362 hands of human and other primates 518–528.
- 363 Vaz, A., Singh, K., Dauphin-Tanguy, G., 2015. Bond graph model of extensor mechanism of  
364 finger based on hook–string mechanism. *Mech. Mach. Theory* 91, 187–208.  
365 <https://doi.org/10.1016/j.mechmachtheory.2015.03.011>
- 366 Wei, Y., Zou, Z., Qian, Z., Ren, L., Wei, G., 2022. Biomechanical Analysis of the Effect of the  
367 Finger Extensor Mechanism on Hand Grasping Performance. *IEEE Trans. Neural Syst.*

368 Rehabil. Eng. 30, 360–368. <https://doi.org/10.1109/TNSRE.2022.3146906>

369 Zancolli, E., 1979. Structural and Dynamic Bases of Hand Surgery. J.B. Lippincott Company,

370 Philadelphia; Toronto.

371